DEFORMATION OF POROUS IMPERFECTIONS RELEVANT TO DUCTILE FRACTURE

R. D. Thomson and J. W. Hancock

James Watt Engineering Laboratories, University of Glasgow, Scotland

ABSTRACT

Failure due to hole coalescence initiates in regions where the local concentration of voids is greater than average. Such a region can be regarded as a porous imperfection embedded in a less porous matrix. The stress and strain fields around such an imperfection are examined using a dilating plastic finite element technique to determine the local void growth rates and deformation within the imperfection in uniaxial tension.

KEY WORDS

Ductile failure, dilating plasticity, void growth

INTRODUCTION

Homogeneous plastic deformation can be terminated by the localisation of the plastic strain, which leads to failure with very little additional remote strain. Rudnicki and Rice (1975) have provided the most complete analysis of this process for a dilating continuum, taking the view that it can be regarded as a bifurcation in the homogeneous flow field without the necessity of modelling the interaction of discrete voids which lead to ductile failure. Rice (1976) however has noted that with realistic average porosities the predicted bifurcation strain is too high to be directly responsible for failure. This may be reconciled by noting that failure is likely to initiate in regions where the statistical distribution of inclusions leads to higher than average initial porosities. Yamamoto (1978) idealised such regions as unbounded planar bands of imperfection within the material. These allow homogeneous deformation fields inside and outside the band, while a finite strain discontinuity at the interface permits the deformation rate inside the band to become very much greater than that in the remote field. As a consequence of the strain concentration, the local conditions for unbounded deformation, as defined by Rudnicki and Rice (1975) for within the inhomogeneity, can be met at realistic values of the remote strain.

Inhomogeneities in the form of parallel bands do exist in wrought steels and are a major cause of their anisotropy. However, the unbounded planar inhomogeneities of Yamamoto (1978) were not strictly intended to represent features of the metallurgical microstructure but were a formality by which inhomogeneities could be envisaged at all possible orientations, with localisation occurring at the most favourable angle. The inhomogeneities which occur in the microstructure of real materials are generally better represented in the form of small volumes of highly porous material completely surrounded by material of average porosity than as infinite planar bands. Such inhomogeneities permit stress and strain gradients inside and outside the patch while the deformation within the patch is severely constrained by the surrounding material.

Such an inhomogeneity may be represented by an array of discrete voids with less than average separation embedded in a field of voids of average spacing. Alternatively, the porous material may be considered as a dilating plastic continuum with the embedded inhomogeneity represented as a patch of material of greater thancaverage porosity. The latter approach is adopted in the present work in order to determine the local conditions near the inhomogeneity in a range of stress states. In general the identity of the remote strain state is not maintained near an imperfection of arbitrary shape (Hancock and Brown(1983)). In the current work the simpler case of a spherical imperfection in uniaxial loading is considered so that the axisymmetric deformation is maintained both locally in the imperfection and in the remote field. Such an analysis will determine the existence and nature of the strain concentrations inside the imperfection and their influence on the local void growth rates.

NUMERICAL ANALYSIS

The analysis was performed with the MARC finite element program as modified by Rice and Tracey (1969) which models dilating plastic materials on the basis of a development by Parks (unpublished). The program has a finite strain capability based on the analysis of McMeeking and Rice (1975) with the stress and strain fields determined incrementally using the variational principle of Nagtegaal, Parks and Rice (1974) applied over a mesh of dilating isoparametric quadrilateral elements. The matrix was represented by a perfectly-plastic Von Mises yield surface:

$$\phi = (\bar{\sigma}/\sigma_0) - 1 = 0$$

where $\bar{\sigma}$ is the effective stress defined in terms of the stress deviators s_{ij} by the relation:

$$\bar{\sigma}^2 = (3/2)s_{ij}s_{ij}$$

and σ_0 is the yield stress in uniaxial tension. The plastic strain components are determined from the associated flow rule for the Von Mises yield function, ie the Prandtl-Reuss equations. An elastic modulus (E) of 210.0 GPa and a matrix yield stress (σ_0) in uniaxial tension of 0.14 GPa were chosen to give a constitutive response representative of a low yield, non-hardening matrix. The effect of porosity is introduced into the yield surface through a pressure dependent term g to give:

$$\phi = (\bar{Z}/\bar{\sigma})^2 - g(Z_{kk},f) = 0$$

where f is the current void volume fraction, $\bar{Z}$ is defined in terms of the aggregate stress deviators S_{ij} from:

$$\bar{Z}^2 = (3/2)S_{ij}S_{ij}$$

and Z_{kk} is the trace of the aggregate stress tensor. In the light of an original analysis by Gurson (1977), Tvergaard (1982) has suggested that

$$g(Z_{kk},f) = (1 + 2.25f^2) - 3f\cosh(Z_{kk}/(2\bar{\sigma}))$$

Setting f = 0 recovers the Von Mises yield surface for a non-porous material, in which $Z_{ij} = \sigma_{ij}$. For a isotropic material, normality of the matrix deformation implies normality of the aggregate (Bishop and Hill (1951)) and hence the existence of an associated flow rule through the relation:

$$dE^p_{ij} = d\Lambda\,(\partial\phi/\partial Z_{ij})$$

in which the pressure dependence exactly matches the dilation rate, which can be written:

$$dE_{kk}/d\bar{E}^p = (1.5f\sinh(Z_{kk}/(2\bar{\sigma})))/(\bar{Z}/\bar{\sigma})$$

The aggregate flow stress $\bar{Z}$ can be updated from the aggregate deformation and the properties of the non-hardening matrix through the work relationship:

$$Z_{ij}dE^p_{ij} = (1-f)\bar{\sigma}d\bar{e}^p$$

in which the work done by the external stresses is dissipated by incompressible plastic flow in the matrix. The matrix strain $\bar{e}^p$ is then a convenient measure of deformation. Rudnicki and Rice (1975) note the importance of the aggregate hardening rate, defined as:

$$H = (1/\sigma_0)(d\bar{Z}/d\bar{E}^p)$$

which determines of the stability of homogeneous deformation.

ANALYSIS

In order to get a feel for the likely porosities in an inhomogeneity, the Poisson distribution may be evaluated using data appropriate to Swedish Iron which contains a volume fraction of 1% spherical inclusions with an average diameter of 5 μm. Any volume V of material may be partitioned into cells of volume δV which contain on average one inclusion. Attention may now be focussed on a small volume V = 10 mm^3 in the centre of a tensile specimen of such material, where failure initiates. This volume V will contain 1.5×10^6 cells with an 80% probability that at least one cell in V will have an inclusion concentration factor of 10 or more. The numerical values are not critical but there is clearly a high probability of finding inhomogeneities with inclusion concentrations an order of magnitude greater than average.

An inhomogeneity of this nature was modelled by the finite element grid in fig 1 in which the 50 elements in the 5 innermost rings have greater than average porosities. The remote boundary was specified to be at a distance of 6 times the radius of the inhomogeneity. An initial porosity of 11% was specified for the innermost ring with 10% initial porosity for the elements in the 4 adjacent rings. This ensured that yielding initiated at the centre of the patch and that the conditions at the centre were not dominated by the proximity of a sharp interface with the less porous environment.

The finite element model was subjected to increments of displacement loading on the remote boundary (y = constant) up to a final remote uniaxial strain of the order of 30 times the initial yield strain. Contour plots (figs.2,3) of stress and strain quantities show only small gradients both inside the patch and in the remote field, throughout the whole of the loading history although stress and strain gradients are produced near the interface. The sharply defined interface is an extreme case, compared with which a more realistic diffuse interface might be expected to produce less severe deformation gradients. Both locally and in the remote environment, $\bar{e}^p$ developed linearly with the remote strain as shown in fig.4. From this it is apparent that there is little strain concentration within the imperfection although the porosity has a marked effect in relieving the aggregate effective stress Z (fig.5). However, as the hydrostatic stress is also reduced in the same way, the ratio of $Z_{kk}/\bar{Z}$ is relatively insensitive to increasing deformation. The strain concentrations which develop in the environment of the interface aid the propagation of the damage throughout the material. While the porosity increased throughout the field (fig.6), the ratio of the porosity in the patch to the remote porosity remained constant throughout the deformation history (fig.7).

DISCUSSION

The contained porous imperfection analysed in the present work may be regarded as intermediate between an arbitrary volume of average aggregate material and a void, which can be thought of as an imperfection in which the local porosity f = 1. The effect of hydrostatic stress in intensifying the strain concentration and deformation gradients near a single void are well known from the work of Rice and Tracey (1969), McClintock (1968) and Budiansky, Hutchinson and Slutsky (1981), and the porous inhomogeneity shows similar effects whereby increasing triaxiality intensifies the strain gradients close to the interface as well as enhancing the matrix strain concentration and the dilation rate within the inhomogeneity. Not surprisingly, the enhanced porosity of the imperfection has a significant effect in lowering both Z_{kk} and $\bar{Z}$, but in such a way that the ratio of $Z_{kk}/\bar{Z}$ is relatively insensitive to increasing deformation. For this stress state, the normalised void growth rate $df/(fd\bar{E}^p_\infty)$ expressed in terms of the remote strain is the same both in the inhomogeneity and in the remote field. The ratio of the dilations reflects the ratio of the initial void volume fractions at these locations. This growth rate is similar to the value of approximately 1 determined by Budiansky, Hutchinson and Slutsky(1981) for a single void in an infinite, strongly hardening matrix (m = 3). While the need for a simple yield surface may prevent the ideal case being realised exactly, it is natural to find that the growth rates for voids in a porous material with low void volume fractions (f = 0.01), subject to moderate triaxialities, are close to those for a single isolated void in a similar stress state. It is of more significant to note that the enhanced porosities in the imperfection show similar growth rates to those for a single void. The effect of the deformation is to exacerbate the difference in porosity between the imperfection and the remote field so that failure initiates in the imperfection before the surrounding material. For a nonhardening matrix, the hardening rate of the porous aggregate will be negative throughout the deformation history, particularly in the highly porous patch. It is of interest to note the kinematic constraint on the inhomogeneity, exercised by the surrounding average material. This implies that conditions will be locally favourable for void coalescence without such failure occurring over a size scale sufficient to cause immediate macroscopic failure and local perturbations in porosity have an important bearing on the ductile failure process.

REFERENCES

Bishop J F W and Hill R (1951). A theory of the plastic distortion of polycrystalline aggregate under combined stress. Philosophical Magazine, 42, 414-427.

Budiansky B, Hutchinson J W and Slutsky S (1981). Void growth and collapse in viscous solids. Mechanics of Solids, The Rodney Hill 60th Anniversary Volume (ed Hopkins H G and Sewell M J), Pergamon Press, 1981.

Gurson A L (1977). Continuum theory of ductile rupture by void nucleation and growth, Part 1 - Yield criteria and flow rules for porous ductile media. Trans ASME J Eng Mat Tech, 99, 2-15.

Hancock J W and Brown D K (1983). On the role of strain and stress state in ductile failure. J Mech Phys Solids, 31, 1-24.

McMeeking R and Rice J R (1975). Finite element formulations for problems of large elastic-plastic deformation. Int J Solids Structures, 11, 601-616.

Marcal P V and King I P (1967). Elastic-plastic analysis of 2-dimensional systems by the finite element method. Int J Mech Sciences, 9, 143-155.

Nagtegaal J C, Parks D M and Rice J R (1974). On numerically accurate finite element solutions in the fully plastic range. Computer Methods in Applied Mech and Eng, 4, 153-177.

Rice J R and Tracey D M (1969). On the ductile enlargement of voids in triaxial stress fields. J Mech Phys Solids, 17, 201-217.

Rudnicki J W and Rice J R (1975). Conditions for the localisation of deformation in pressure sensitive dilatant materials. J Mech Phys Solids, 23, 371-394.

Tvergaard V (1982). Material failure by void coalescence in localised shear bands. Int J Solids Structures, 18, 659-672.

Yamamoto H (1978). Conditions for shear localisation in the ductile fracture of void-containing materials. Int J Fracture, 14, 347-365.

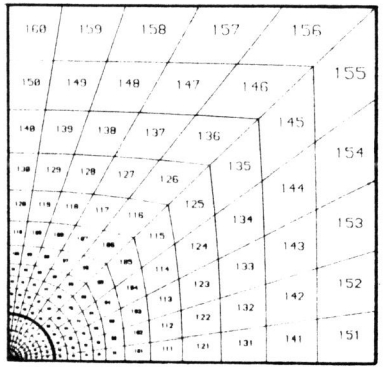

Fig 1. Finite element grid. The imperfection is contained within the five innermost rings.

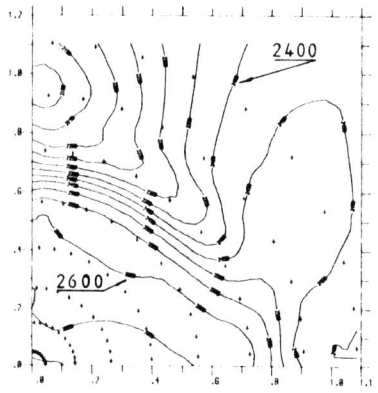

Fig 2. Effective plastic strain in the vicinity of the imperfection ($\bar{e}^p$=24e_0 at contour 2400, $\bar{e}^p_\infty$=24e_0).

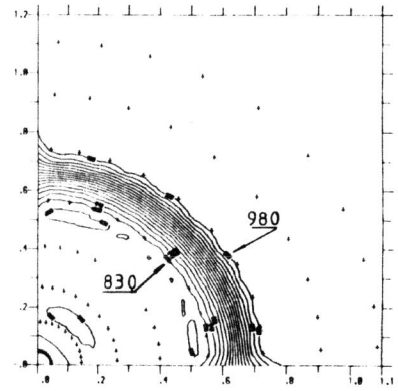

Fig 3. Flow stress in the vicinity of the imperfection ($\bar{Z}$ = 0.98σ_0 at contour 980, $\bar{e}^p_\infty$ = 24e_0).

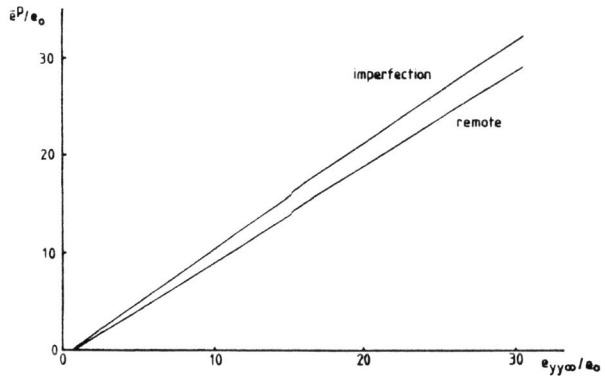

Fig 4. Matrix strain concentration within the imperfection.

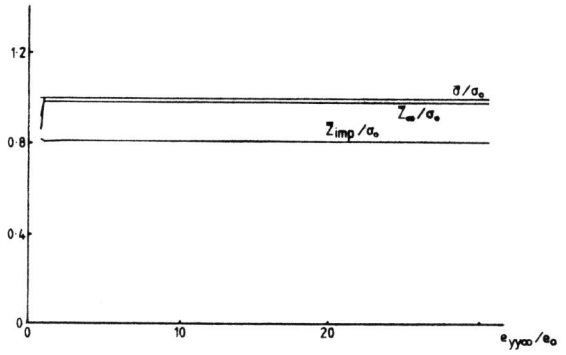

Fig 5. The development of matrix and aggregate effective stresses ($\bar{\sigma}$ and $\bar{Z}$) in the imperfection and in the remote field. For $\bar{\sigma}$, the local and remote curves are collinear.

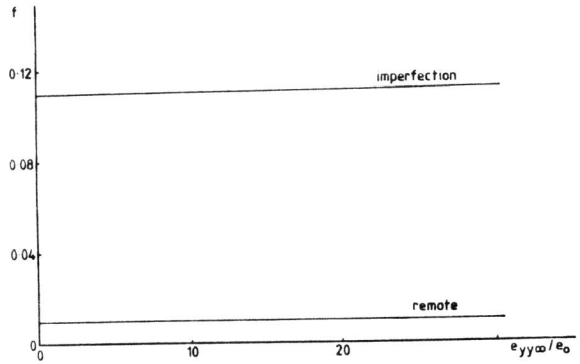

Fig 6. The development of porosity (f) in the imperfection and in the remote field.

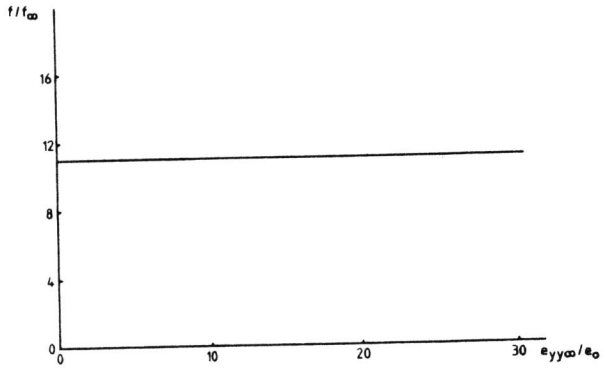

Fig 7. Ratio of local to remote porosity.